

# Chapter 1

## Carbon Nanomaterials for Energy Storage Devices



Zhipeng Wang and Gan Jet Hong Melvin

### 1.1 Introduction

Extreme climate changes and the decreasing availability of fossil fuels, such as coal, natural gas, oil, and so on, require the users, providers, and society to gear towards sustainable and renewable resources (Simon and Gogotsi 2008; Yang et al. 2011). This fact is strongly supported and apparent as the global energy consumption has been speeding up at an alerting rate due to the fast economic expansion worldwide, increase in world population, and the rapidly growing of energy-based appliances including increasing human reliance on them (Dai et al. 2012). For instance, it was estimated that the world need to double its energy supply by 2050 to fulfill the demands (Dai et al. 2012; Chen and Dai 2013).

Accordingly, we can observe the boost in renewable energy production and utilization, for example from sun and wind. However, sun does not shine during the night and wind does not blow on request, which means that power generation does not necessarily correspond to demand. Furthermore, it is worth to concern that the renewable resources are localized and often away from the load centers (Yang et al. 2011). Moreover, it is undeniable that fossil fuels, nuclear heat, renewable energies are available to be converted to electrical energy. However, this conversion is performed with large energy losses, for instance only about 30% of the nuclear heat is converted to electrical energy (Fauvarque and Simon 2010). Thus, energy storage systems play a significant role and essential in our lives, to prevent

---

Z. Wang

Institute of Advanced Materials, Jiangxi Normal University, Nanchang, Jiangxi Province, China

G. J. H. Melvin (✉)

Material and Mineral Research Unit (MMRU), Faculty of Engineering, Universiti Malaysia Sabah, Jalan UMS, Kota Kinabalu, Sabah, Malaysia

e-mail: [melvin.gan@ums.edu.my](mailto:melvin.gan@ums.edu.my)

© Springer Nature Switzerland AG 2019

S. Siddiquee et al. (eds.), *Nanotechnology: Applications in Energy, Drug and Food*,  
[https://doi.org/10.1007/978-3-319-99602-8\\_1](https://doi.org/10.1007/978-3-319-99602-8_1)

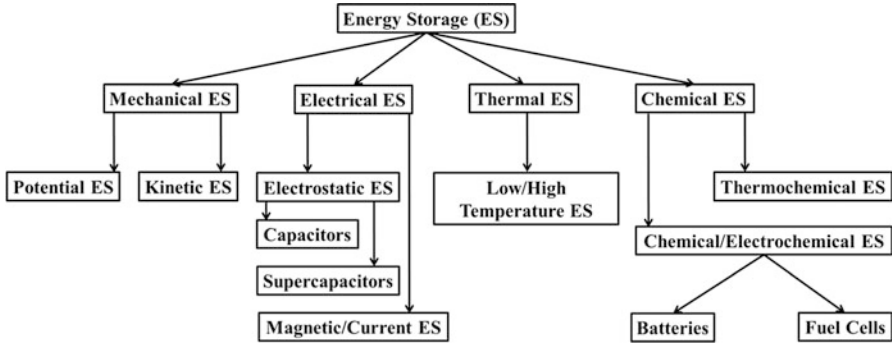


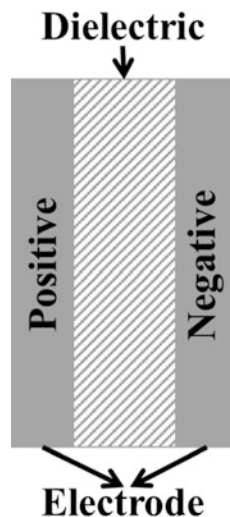
**Fig. 1.1** Various types of energy storage technology

unnecessary losses and supplying necessary energy which satisfies the demands. From this point of view, electrical energy storage systems such as batteries and electrochemical capacitors (ECs) have been studied extensively and becoming the center of highlight for this particular reason. Majorly, energy storage can be divided into chemically, electrochemically, and electrically stored (Pumera 2011). The classification of major energy storage technologies is presented in Fig. 1.1.

In our daily life, batteries are one of the most common electrical energy storage devices owing to their capability to store large amount of energy in a relatively small volume and weight, and in the same time are able to provide appropriate and suitable levels of power for wide broad applications. However for batteries, even though high energy densities can be obtained, slow power delivery has agonized them (Zhai et al. 2011). This is one of the reasons which limited or restricted their utilization, especially when fast storage coupled with high power is the demands. Alternatively, to tackle the constraints, ECs or usually described as supercapacitors or ultracapacitors have been given the attentions. Some of the benefits of ECs are, they can provide high specific power, a long cycle life, fast charge/discharge process, and so on (Zhai et al. 2011). However, within seconds charge/discharge process of ECs caused their energy density is lower than the batteries, but faster power delivery can be accomplished in short time (Simon and Gogotsi 2008, 2013). ECs play an essential role in complementing or substituting batteries in the energy storage field, for example they can act as back-up power supply utilized to protect against power disruption, load levelling, and so on (Simon and Gogotsi 2008; Zhai et al. 2011).

Generally, electric capacitor is a sandwich structure of several materials, where two conductive plates neighboring a dielectric/insulator, as illustrated in Fig. 1.2. The charge accumulation will occur during charging process and the charge separation will occur during discharging process (Yu et al. 2013). They can be divided into electrostatic and electrolytic (utilization of electrolytes as dielectrics) capacitors which are considered as the first and second generation capacitors. These capacitors function mainly as the components in electrical circuit to store micro- to picofarad charges of direct current or to filter the frequencies for alternating current circuits. Rapid progress in materials science, advancement of technologies, and high

**Fig. 1.2** Conventional electric capacitor



demands are some of the factors that lead to the invention of third generation, supercapacitors.

Capacitive behavior of ECs can be majorly categorized into two types, depending on their charge storage mechanism and active materials utilized. First type is the electrochemical double layer capacitors (EDLCs), where active materials with high surface area are ideal and dependent on electrostatic attraction between ions and the charged electrode's surface or electrostatic charge accumulation at the electrode/electrolyte interface (Simon and Gogotsi 2008; Chen and Dai 2013; Zhai et al. 2011). Carbon materials are one of the prominent candidates to be selected as the active materials (He et al. 2017). Second type is redox supercapacitors or also known as pseudo-capacitors, which is highly associated with fast redox or Faradaic charge transfer reactions of the electro-active materials, such as metal oxides (Wallar et al. 2017) or conducting polymers (Jo et al. 2017), on the surface of the electrodes, for charge storage (Simon and Gogotsi 2008; Zhai et al. 2011; Yu et al. 2013). It is also worth to notice the existence of hybrid capacitors that combine the capacitive or pseudo-capacitive electrode with a battery electrode, which integrate the properties of both, capacitor and battery. The classification of various supercapacitors is presented in Fig. 1.3.

The earliest EC with extinguish high capacitance was described and patented in 1957 by Becker (Becker 1957). Carbon with a high specific surface area coated on a metallic current collector in a sulphuric acid solution was utilized. In 1966, Standard Oil of Ohio (SOHIO) developed another version and patented a device that stored energy in double layer interface (Rightmire 1966). Advancing with further adjustments, Boos invented the first practical supercapacitor and patented in 1970 (Boos 1970). Then in 1971, Nippon Electronic Company (NEC), Japan, licensed the technology from SOHIO and developed aqueous-electrolyte capacitors for powersaving units in electronics, and this application can be reflected as the pioneer

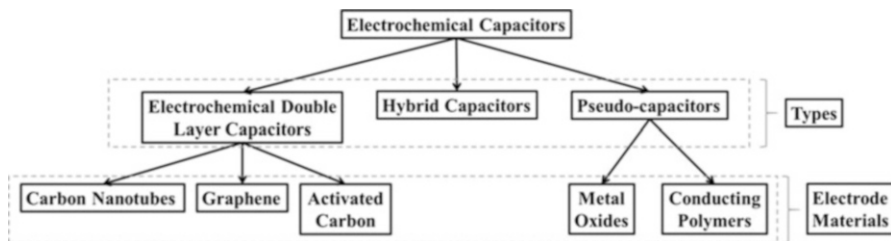


**Fig. 1.3** Classification of various supercapacitors

for EC utilization in commercial products (Simon and Gogotsi 2008; Sharma and Bhatti 2010).

Typical ECs or supercapacitors use electrolyte solutions but have even greater capacitance per unit volume due to their porous electrode structure compared to electrostatic and electrolytic capacitors. They are constructed with three essential components, namely the electrodes, the electrolyte, and the separator. The overall performance of supercapacitors is determined by the physical properties of both the electrode and the electrolyte materials. Nevertheless, the electrode is one of the most important components for charge storage/delivery, and plays a vital role in determining the energy and power densities of a supercapacitor. The electrochemical performance of a supercapacitor can be characterized by cyclic voltammetry and galvanostatic charge-discharge measurements. Furthermore, ECs are categorized into two major groups, which are symmetric and asymmetric (Sharma and Bhatti 2010). Symmetric ECs (SECs) use the similar electrode material (usually carbon) for both the positive and negative electrodes. Asymmetric ECs (AECs) use two different materials for the positive and negative electrodes. SECs get their electrostatic charge from the accumulation and separation of ions at the interface between the electrolyte and electrodes. Aqueous or organic electrolyte solutions can be utilized for SECs. The electrolyte solution comprises aqueous substances (such as potassium hydroxide or sulfuric acid) or organic substances (such as acetonitrile or propylene carbonate). An SEC using aqueous electrolyte is also known as a Type I SEC and an SEC using organic electrolyte is known as a Type II SEC. Similarly, an AEC using an aqueous electrolyte is known as a Type III AEC and one using organic electrolyte is known as a Type IV AEC. A typical charge storage mechanism of electrochemical double-layer capacitor (EDLC) is depicted in Fig. 1.4.

It is undeniable that nanomaterials, especially carbon nanomaterials play a great role in the development of ECs. This is due to their remarkable structure, electrical properties, electrochemical stability, and so on. High performance and functionality can be expected from carbon nanomaterial-based ECs. In this chapter, the influence factors of EC performance focusing on graphene and carbon nanotubes (CNTs) will be discussed further.

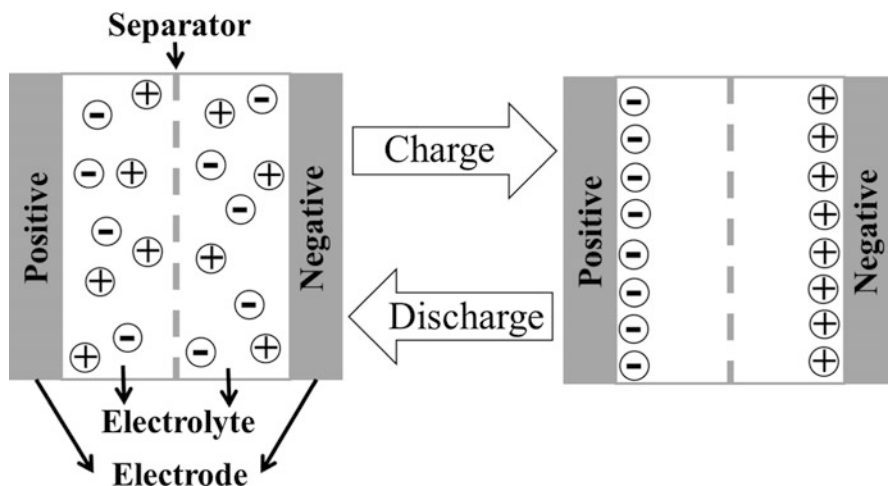


Fig. 1.4 Charge/discharge process of electrochemical double-layer capacitor

## 1.2 Carbon Nanomaterials

### 1.2.1 Carbon Nanotubes

There are great numbers of reviews and publications related to the history, synthesis, excellent properties, and development as ECs of CNTs. Since the discovery of fullerene ( $C_{60}$ , buckyball) by Kroto et al. (1985), among the first synthesis of CNTs by Oberlin et al. (1976), observation of both multi- and single-walled CNTs soon afterwards by Iijima in 1991 (Iijima 1991) and 1993 (Iijima and Ichihashi 1993), respectively, the interest in CNTs has rapidly developed. Furthermore, CNTs are famous for their outstanding mechanical, electrical, chemical, thermal, etc. properties that allow them to be manipulated for various applications and research studies.

Generally, CNTs can be grouped into single-walled CNT (SWCNT) and multi-walled CNT (MWCNT). A SWCNT can be thought of as a rolled-up sheet of a structure called graphene, which is a single layer of an allotrope of carbon called graphite, and the edges of the sheet are joined together to form a seamless tube (Young and Lovell 2011; Hierold et al. 2008). Several tubes of different diameters can be fitted into each other to make a MWCNT. Figure 1.5 shows the images of CNT and graphene.

There are mainly three methods to produce CNTs: arc discharge, laser ablation, and chemical vapor deposition (CVD). Each of these techniques had its advantages and disadvantages and briefly discussed below.

Arc discharge and laser ablation depend on the evaporation of a graphite target to create gas phase carbon fragments that recombine to form CNTs. The temperature

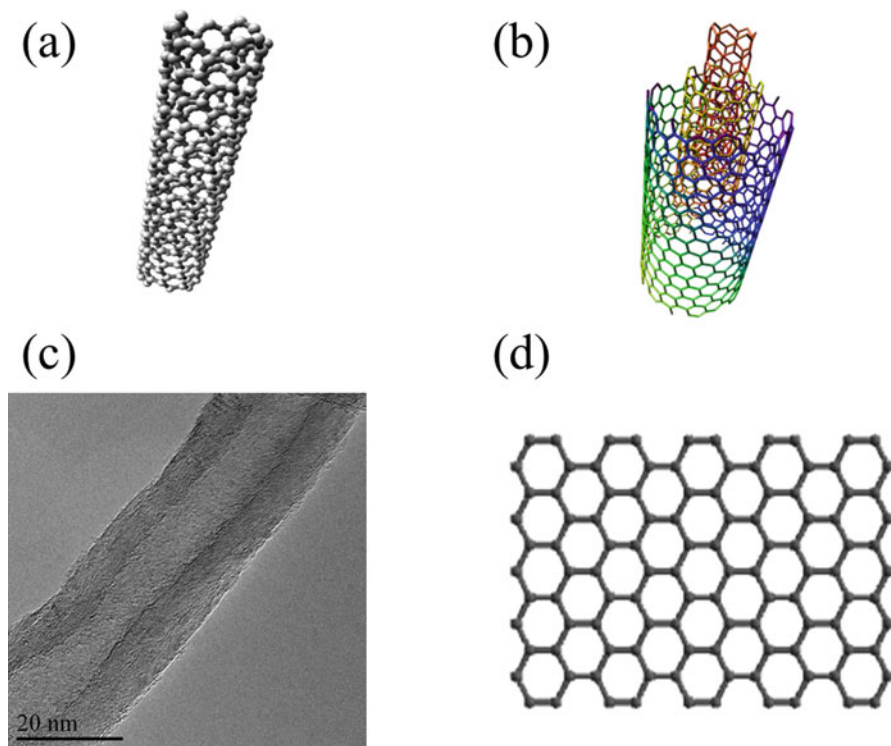


**Fig. 1.5** (a) SWCNT, (b) MWCNT, (c) TEM image of MWCNT, (d) graphene

reached in these processes is in the range 2000–3000 °C, more than sufficient for the carbon atoms to rearrange into the tube structure. In order to promote the yield of CNTs, several different metals in concentrations about 1% are incorporated into the target materials that is evaporated (Hierold et al. 2008). For application of CNTs for composite materials where large quantities of CNTs are required, these methods would make the cost of CNTs prohibitive (Thostenson et al. 2001). However, a large amount of non-tubular graphitic and amorphous carbon is also produced during the process (Hierold et al. 2008; Thostenson et al. 2001). Thus, purification steps are essential before the usage of them.

CVD is the most widely used method for the production of CNTs. Generally, the CVD process includes catalyst-assisted decomposition of hydrocarbons, usually ethylene or acetylene, in a tube reactor at 400–1100 °C and growth of CNTs over the catalyst upon cooling the system (Hierold et al. 2008; Hu et al. 2010; Popov 2004). The growth temperature depends on the type of CNTs to be grown and the catalyst composition (Hierold et al. 2008). The advantages of this method are the ability to fabricate aligned arrays of CNTs with controlled diameter and length, and under the right condition only nanotubes are produced and no unwanted graphitic material (Hierold et al. 2008; Thostenson et al. 2001).

## 1.2.2 Graphene

Since the extraction of graphene from bulk graphite in 2004 (Novoselov et al. 2004), which this discovery was recognized by Nobel Prize in Physics (2010), the interest in graphene has rapidly increased. In that study, graphene sheets were obtained by using Scotch tape to repeatedly split graphite crystals into increasingly thinner pieces until individual atomic planes (monolayer of graphite) were reached. Graphene is a one-atom-thick planar sheet of two-dimensional (2D) sheet  $sp^2$  bonded carbon atoms that are densely packed in a honeycomb crystal lattice. As the mother and components of all graphitic forms, graphene is a building block for carbon materials of all other dimensionalities, for instance 0D buckyballs, 1D nanotubes, and 3D graphite. Graphene, in fact, including multi-layered graphene, possesses high aspect ratio, large surface area, excellent electrical, thermal, mechanical properties, and so on (Dai et al. 2012; Pumera 2010).

Generally, preparation of graphene can be categorized into top-down and bottom-up approaches. Several factors are to be considered in graphene preparation, such as cost effectiveness, scaled-up production, high electrochemical activity, conductivity, and so on (Lv et al. 2016).

Top-down approach usually utilizes mechanical force or chemical intercalation to overcome the van der Waals forces between the graphene layers to achieve separation of graphene from bulk graphite, such as micromechanical cleavage (mechanical exfoliation), oxidation-exfoliation-reduction, intercalation exfoliation, solid exfoliation, and so on (Lv et al. 2016; Dong et al. 2017). Particularly for EC applications, mechanical exfoliation by Scotch tape is inappropriate because of the low yield, even though the graphene produced possesses high quality (without abundant defects).

Bottom-up approach usually utilizes a small molecule precursor to grow into graphene by chemical vapor deposition (CVD) or chemical synthesis. For graphene prepared by CVD, they show some excellent properties, as a result of their large crystal domains, monolayer structure and less defects in the graphene sheets, which are beneficial for boosting carrier mobility in electronic applications (Ke and Wang 2016). Furthermore, the layers and defects of graphene can be controlled by adjusting growth parameters such as temperature, time, catalyst, and so on.

By utilizing physical or chemical method appropriately, preparation of porous graphene and doped graphene sheets can be realized, and high performance/functionality graphene can be prepared with introduction of organic/inorganic materials. In the same time, the production of graphene with low cost, high yield, and high quality is also a crucial factor. Generally, the chemical exfoliation of graphite into graphene oxides (GOs), followed by controllable reduction of GOs (with reduction agent such as hydrazine hydrate) into graphene can be considered as an efficient and low-cost method (Dong et al. 2017).

### ***1.2.3 Carbon Nanomaterials Derived from Waste Materials***

Carbon nanomaterials such as CNTs and graphene have been utilized widely for the development of ECs due to their exceptional properties. Not limited to chemical process or reaction to obtain carbon nanomaterials, carbonization of waste materials, which is comparatively low cost and environment friendly, can be considered as a beneficial method (Melvin et al. 2017a, b). Since most of the waste materials are available in large scale, greener technology to produce bulk quantity of valuable carbon nanomaterials from waste materials can be promoted. Waste materials can be in the form of agricultural wastes, synthetic compound wastes, and so on.

Agricultural waste materials, such as rice husks, have been exploited to produce carbon nanomaterials (Muramatsu et al. 2014; Wang et al. 2015). A good quality of carbon nanomaterials (graphene, derivatives of graphene) can be obtained. They offer high performance and promising applications in carbon-based energy storage and conversion devices.

Furthermore, through chemical or physical activation of carbon materials derived from waste materials, activated carbon (AC) can be produced. ACs are usually used due to their porous structure that can lead to high capacitance, which is favorable in ECs field. Some of the recent reports, activated carbon are produced from corn straws (Lu et al. 2017), oil palm shells (Abioye et al. 2017), sawdusts (Huang et al. 2017), which are dedicated to the development of high performance ECs.

## **1.3 Influence Factors of Energy Storage**

### ***1.3.1 Porosity Effect***

A simplest model of an EC is composed of two pieces of conductive electrodes (mainly porous carbon materials) with high-surface-area porous structures, which were soaked into electrolyte and separated by an ion-conducting but electron-insulating separator membrane (Conway 1999). The two electrodes are identical for a symmetric supercapacitor, but different for an asymmetric supercapacitor (ASC). By applying voltage to the two electrodes, the electrolyte ions with the opposite signs accumulate on the surface of each electrode, and the concentration of ions is commonly proportional to the applied voltage. For EDLC, the capacitance originates from the pure electrostatic charge adsorption on the interface between electrode and electrolyte. Therefore, the capacitance is strongly dependent on the surface area of the electrode materials which is accessible to the electrolyte ions. The porous carbon materials with large surface area enable EDLC to possess high capacitance. As for pseudo-capacitor, it involves chemical and electrochemical interactions with the electrolyte. These interactions with fast and reversible Faradaic processes provide additional charge storage, resulting in higher energy densities for the ECs. When an EC stores charges by a capacitive carbon electrode with a



pseudocapacitive electrode, it is then called a hybrid supercapacitor. Due to their excellent physiochemical properties as well as controllable structures and relatively low costs, porous carbon materials have been widely used as the electrode materials in all types of ECs.

The energy density of ECs is determined by the capacitance of their electrodes and the operating maximum voltage. The EC energy could be calculated according to following equation (Gu and Yushin 2014):

$$E = \left( \frac{C_- \cdot C_+}{C_- + C_+} \right) \cdot V_{\max}^2 \quad (1.1)$$

where  $E$  is the energy,  $V_{\max}$  is the maximum voltage between two electrodes,  $C_-$  and  $C_+$  are the capacitances of the negative and positive electrodes, respectively. When the capacitances of the both electrodes are the same, the maximum energy is achieved:

$$E = \frac{C \cdot V_{\max}^2}{2} \quad (1.2)$$

In a symmetric EDLC, the specific capacitance of each electrode could be identified by a galvanostatic charge-discharge measurement, where the specific capacitance is determined by the following equation:

$$C = Idt/dV \quad (1.3)$$

The power density is another crucial parameter for evaluating the EC performance, and can be obtained using equation:

$$P = \frac{V_{\max}^2}{4R} \quad (1.4)$$

where  $P$  is the power density,  $R$  is the equivalent series resistance including intrinsic resistance of electrode materials, contact resistance between the electrode materials and current collectors, diffusion resistance of ions in electrode materials and through the separator, and ionic resistance of electrolytes.

One strategy to improve the energy density of EDLC is to maximize the capacitance, which is affected by not only specific surface area (SSA), but also pore size and distribution, pore volume, and electrical conductivity. Initially, it was expected that the larger SSA, the higher capacitance. Thus, most efforts have been focusing increasing the specific capacitance of EDLCs by increasing the SSA of carbon materials. However, it was found that the specific capacitance of carbons increases with increasing SSA at relatively low values, but it rapidly tends to saturation when the SSA is greater than 1200–2000 m<sup>2</sup> g<sup>-1</sup> (Barbieri et al. 2005). It means that there is no linear relationship between the SSA and the capacitance. For example, ACs

with SSA as high as 2500–3000 m<sup>2</sup> g<sup>-1</sup> possessed a relatively small capacitance of less than 10 μF cm<sup>-2</sup>, which is smaller than the theoretical capacitance of EDLCs (15–25 μF cm<sup>-2</sup>) (Raymundo-Piñero et al. 2006). On the contrary, activated carbon fibers with a SSA of nearly 1000 m<sup>2</sup> g<sup>-1</sup> (i.e., 730–1274 m<sup>2</sup> g<sup>-1</sup>) show extremely high capacitances corresponding to those for conventional AC materials with a SSA of 3000 m<sup>2</sup> g<sup>-1</sup> (Kim et al. 2012). Obviously, the wrong impression was almost given when the SSA was employed to discuss the capacitance of EDLC electrodes which were made of activated carbon materials. Recently, many attempts have been made to investigate the relationship between the porosity and the capacitance of carbon materials. The results showed that an appropriate pore is more important than a high SSA to achieve high capacitance performance. As we know, based on the International Union of Pure and Applied Chemistry (IUPAC) classification, pore sizes can be classified into three types: micropores (<2 nm), mesopores (2–50 nm), and macropores (>50 nm). Previous studies showed most of the surface area of AC electrode materials locates in the scale of micropores (Frackowiak and Béguin 2001). These pores are often poorly or non-accessible for electrolyte ions, especially for organic electrolytes, and are not suitable for forming an electrical double layer on the pore walls. However, Chmiola et al. (2006a) reported that the ion solvation shell will be highly distorted and can further enter the micropores, resulting into an anomalous increase in the capacitance for carbon materials with pore sizes less than 1 nm, as shown in Fig. 1.6. In the related research, carbide-derived carbon with pore sizes of 0.8–1.0 nm also showed high specific surface capacitance in 1 M H<sub>2</sub>SO<sub>4</sub> due to the desolvation of the electrolyte ions entering subnanometer pores, which cause a sieving effect at pore sizes less than the solvated ion sizes (Chmiola et al. 2006b). The same group further investigated the relation between the ion size and pore size for the EDLC application using solvent-free electrolyte, e.g. ionic liquid (IL), and demonstrated a maximal normalized capacitance at the pore size of about 0.7 nm, which is nearly close to the electrolyte ion sizes (Largeot et al. 2008). The similar results were also concluded in the organic electrolytes (Segalini et al. 2012). These interesting finds challenged the long-term ideals that only pores with size bigger than that of solvated electrolyte ions can contribute to the capacitance of EDLC. In fact, it has been reported that mesopores contribute the most to the capacitance in the EDLCs (Tanahashi et al. 1990). Very recently, Lin et al. obtained the high specific capacitance from nitrogen-doped mesoporous carbon with a bimodal pore size distribution centered around 1.8 nm and 3.5–4 nm in all three mesoporous structures (Lin et al. 2015). However, the straight mesoporous channels are only effective for a fast transportation of electrolyte ions to the small micropores where they are stored (Vix-Guterl et al. 2005). Therefore, the relation between the pore size and capacitance should be future investigated both theoretically and experimentally, which is propitious to design the carbon materials for EC electrodes with high performance.

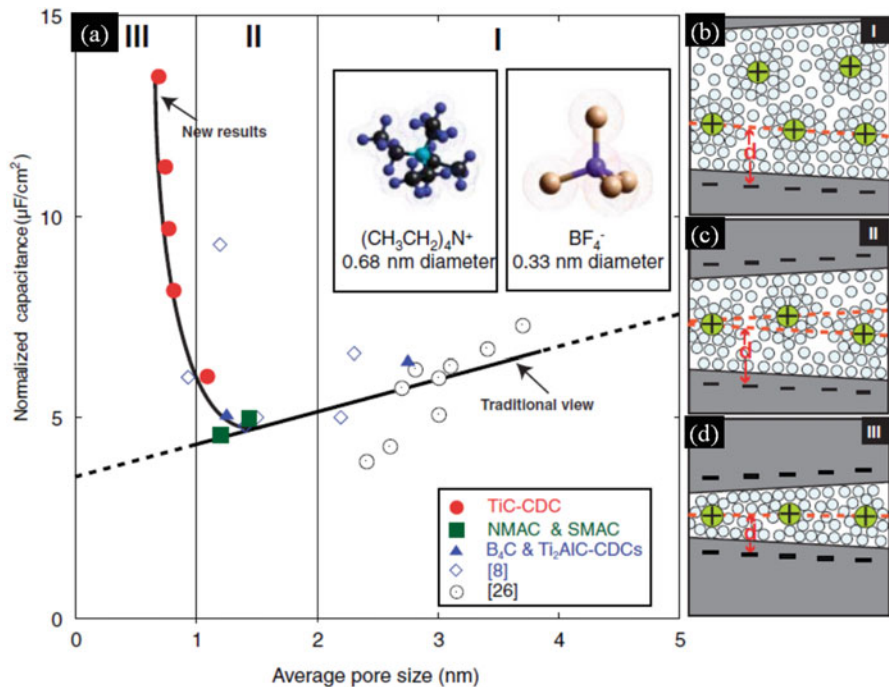


**Fig. 1.6** (a) Specific surface capacitance normalized by BET SSA for carbide-derived carbon vs average pore size shows an increasing trend with decreasing pore size below 1 nm. Diagrams of solvated ions residing in pores with distance between adjacent pore walls: (b) greater than 2 nm, (c) between 1 and 2 nm, and (d) less than 1 nm demonstrate this behavior schematically (Chmiola et al. 2006a)

### 1.3.2 Electrolyte Effect

According to Eq. (1.2), besides improvement of capacitance of the electrode materials, an alternative strategy to increase the energy density is enlarging the applied voltage, which is strongly dependent on the selected electrolyte. As an ideal electrolyte for ECs, it should be satisfied with some features as follows: high ionic conductivity, low viscosity to access small pores, chemical inertness (no reaction with the electrode materials), well-matched with the electrolyte materials, a low volatility and flammability, and low cost. Currently employed electrolytes in ECs include aqueous, mostly H<sub>2</sub>SO<sub>4</sub>, KOH, and Na<sub>2</sub>SO<sub>4</sub>, organic, mostly acetonitrile (ACN), and propylene carbon (PC), and ionic liquid electrolytes. The typical characteristics of electrolyte, e.g. ion type and size, the ion concentration and solvent, and the interaction between the ion and the solvent, play important roles in the EDLC capacitance and pseudocapacitance. The electrochemical stability of electrolyte affects directly the maximal operation voltage of an EC, and further

determines the energy and power densities of the EC. The aqueous electrolytes have high conductivity and small ion size, which easily penetrates inside small pores to access high surface area. However, due to the aqueous electrolyte's potential window of 1.23 V (water decomposition voltage is 1.23 V at 1.0 atm and room temperature), the aqueous electrolyte-based ECs have usually an operating potential window of around 1.0–1.3 V. Certainly, the operation voltage of aqueous electrolytes is strongly dependent on their pH values. High  $\text{H}^+$  or  $\text{OH}^-$  concentration, e.g.  $\text{H}_2\text{SO}_4$  or  $\text{KOH}$ , would limit the voltage window. Compared to counterparts, neutral electrolytes with low  $\text{H}^+$  or  $\text{OH}^-$  have higher operating voltage and can be increased by appropriate doping of the electrode materials. For instance, the voltage window of 2.0 V from aqueous  $\text{Na}_2\text{SO}_4$  electrolyte was achieved due to the electro-oxidation of  $\text{H}_2$  absorbed in CNTs with high oxygen content and disorder (Hsu et al. 2012). A higher operating voltage of 2.4 V in the  $\text{Na}_2\text{SO}_4$  electrolyte was reported for N-containing carbon electrodes by Bichat et al., suggesting that surface functionality strongly affects the over-potential of di-hydrogen evolution and carbon oxidation (Bichat et al. 2010).

The organic electrolyte-based and IL-based ECs generally have potential windows of 2.5–2.7 V and 3.5–4.0 V, respectively, which are higher than aqueous electrolyte-based ECs (Zhong et al. 2015). However, organic electrolytes have low conductivity and larger ion size, which results into power deterioration and low capacitance. Besides those, other issues such as complex purification procedure, safety concerns (flammability), volatility as well as toxicity also exist for organic electrolytes. ILs, known as room temperature molten salts, are nonflammable, which is important for many mobile electronic devices and hybrid vehicles. Besides this, ILs have other advantages including high electrochemical stability, high electrochemical stability over a wide potential window, non-toxicity, and various combination choices of cations and anions. But, ILs have typically high current cost, high viscosity liquids, and low ionic conductivity at room temperature, which limits the charge/discharge rate of IL-based EDLCs.

As for the development of EC electrolytes, widening the potential window of the electrolyte materials can effectively improve the energy density as seen from the Eq. (1.2). It is worth to notice that increasing the applied voltage of ECs would be more efficient than increasing the electrode capacitance in terms of energy density improvement, ascribing to the energy density is proportional to the square of the applied voltage. Thus, developing electrolytes with wide potential windows should be given even higher priority efforts than the development of electrode materials with high capacitance.

Besides the potential window of electrolytes, the interaction between the electrolyte and the electrode materials should be attended because it plays a critical role in the EC performance. As mentioned above, the electrolyte ion size and the pore size of porous carbon materials should be matched for increasing the specific capacitance of EDLCs. The pseudo-capacitors which were composed of carbon-based materials and metal oxides/hydroxides are also affected by the properties of the electrolytes. The internal resistance of ECs is strongly dependent on the ionic conductivity of the electrolytes especially for organic and IL electrolytes. In addition, the operating

temperature and life time of the ECs are heavily influenced by thermal stability of electrolytes, e.g. viscosity, boiling point, and freeze point, and electrochemical decomposition of the electrolytes.

## 1.4 Carbon Nanomaterials for Supercapacitor Applications

Until now, carbon family has many members including from traditional diamond, graphite, activated carbons (ACs) to novel nanocarbons, which contain fullerene, CNTs, graphene, and their derivatives. Previously, AC, a form of disordered carbon (amorphous carbon), has been widely used electrode materials in ECs due to their high surface area, relatively excellent electric properties and low cost. ACs are generally produced by thermal decomposition and physical or chemical activation of carbonaceous sources, including biomass, petroleum coke, and phenolic resins. However, due to wide and random distribution of pore sizes produced by the activation process, ACs only exhibited the limited performance in ECs.

With the successive discovery of fullerene  $C_{60}$ , CNTs, and graphene; carbon nanomaterials have attracted great interest from basic theoretical studies to practical applications. Fullerene  $C_{60}$ , a soccer-like structure, is a perfect electron acceptor, and fullerene and its derivatives have been widely used in solar cells for charge separation. Compared to fullerene, CNTs, graphene, and their composites have been extensively studied as the electrode materials in the energy storage because of their excellent physiochemical properties, e.g. high conductivity, high surface area, and electrochemical activity.

Currently, the hottest topics of research and development on energy storage mainly focus on lithium ion batteries and ECs. Compared to the counterparts, ECs have some advantages of higher power density, longer cyclic stability, higher Coulombic efficiency as well as faster full charge-discharge cycles.

### 1.4.1 Carbon Nanotubes in Electrochemical Capacitors

Due to their unique properties such as good mechanical, thermal stability, high specific surface area, high conductivity, high porosity, high charge transport capability, and high electrolyte accessibility, CNTs have attracted great interest in electrode materials for developing high-performance ECs. According to the published papers, the specific surface area of pure CNTs has been achieved in the range of  $120\text{--}500\text{ m}^2\text{ g}^{-1}$  with the specific capacitance ranging from 2 to  $200\text{ F g}^{-1}$  (Yang et al. 2015). Initially, Niu et al. reported that MWCNT-based supercapacitor electrode, in which MWCNTs are about to be  $\sim 20\text{ }\mu\text{m}$  in length and 8 nm in diameter, exhibited a high specific capacitance of  $102\text{ F g}^{-1}$  with surface area of  $430\text{ m}^2\text{ g}^{-1}$  and a power density of  $8\text{ kW kg}^{-1}$  in concentrated (38 wt%)  $\text{H}_2\text{SO}_4$  aqueous electrolyte (Niu et al. 1997). Frackowiak et al. employed the MWCNTs

with 10–20 nm outer diameters and 2–5 nm inner diameters as supercapacitor electrodes in 6 M KOH electrolyte to achieve BET SSA in the range of 128–411 m<sup>2</sup> g<sup>-1</sup> with the specific capacitances of 4–80 F g<sup>-1</sup>, which are remarkably dependent of the CNT diameters (Frackowiak et al. 2000). Obviously, the diameter of the CNTs plays an important role in affecting the intrinsic surface area.

Generally, SWCNTs have higher SSA than MWCNTs, and will provide higher specific capacitance although they always tend to bundle. An et al. utilized the SWCNT bundles with a diameter of 10–20 nm as the electrode materials in a solution of 7.5 N KOH, and obtained a specific capacitance of 180 F g<sup>-1</sup>, power density of 20 kW kg<sup>-1</sup>, and energy density of 7 Wh kg<sup>-1</sup>, respectively (An et al. 2001). Aligned CNTs may also offer higher SSA than misaligned CNTs. For example, a SWCNT forest was synthesized using the zipping effect of water, which allowed the bulk materials to remain their intrinsic properties, and preserves the high BET SSA of 1000 m<sup>2</sup> g<sup>-1</sup>. The specific capacitance of these aligned SWCNT electrode reached 80 F g<sup>-1</sup> with an energy density of 35 Wh kg<sup>-1</sup> in TEATFB-based organic electrolyte (Futaba et al. 2006).

Besides the structure modulation of CNTs, many efforts have been devoted to improve the specific capacitance of CNTs by increasing their specific surface area via chemical activation (KOH) or plasma treatment. A chemically-activated MWCNTs showed that the BET SSA reach 1050 m<sup>2</sup> g<sup>-1</sup> with the specific capacitances of 90 F g<sup>-1</sup> and 65 F g<sup>-1</sup> in the solution of 6 M KOH electrolyte and 1.4 M TEATFB-based organic electrolyte, respectively (Frackowiak et al. 2002). Another KOH-activation of MWCNTs present the positive results that the BET SSA increased from 194 to 510 m<sup>2</sup> g<sup>-1</sup> with a corresponding increasing of the specific capacitance from 25 to 50 F g<sup>-1</sup> in a LiClO<sub>4</sub>-based organic electrolyte (Jiang et al. 2002).

Plasma treatment has some advantages on CNTs for energy storage such as defect production and functionalization, which makes the modified CNTs more hydrophilic because of functional groups, and results in the improvement of specific capacitance (Yoon et al. 2004). Yoon et al. grew vertically aligned MWCNTs on Ni foil substrate using hot filament plasma enhanced chemical vapor deposition, and modified them by ammonia plasma with the substrate temperature of 650 °C (Yoon et al. 2004). The results demonstrated that the plasma etching causes the MWCNT supercapacitor electrodes in 6 M KOH with increasing BET SSA from 9.6 to 86.5 m<sup>2</sup> g<sup>-1</sup>, and the specific capacitance from 37 to 207 F g<sup>-1</sup>, respectively (Yoon et al. 2004). The similar high performance of supercapacitor electrodes, which were composed of O<sub>2</sub> plasma-activated MWCNTs, has been achieved by Dai group (Lu et al. 2009). Figure 1.7 shows that the vertically aligned MWCNTs were synthesized on Si/SiO<sub>2</sub> by thermal chemical vapor deposition process, and were etched by O<sub>2</sub> plasma to result in opening of the CNT tips, increasing the SSA to 400 m<sup>2</sup> g<sup>-1</sup>, and high specific capacitance of 400 F g<sup>-1</sup> with a high energy density of 148 Wh kg<sup>-1</sup> in the electrolyte of ionic liquid [EMIM][Tf<sub>2</sub>N] (Lu et al. 2009). Recently, the MWCNT powders were treated by microwave and O<sub>2</sub> plasma induced by a radio frequency of 13.56 MHz for enhancing the capacitance of MWCNT electrode (Dulyaseree et al. 2016). The contact angle of droplet of 1 M Na<sub>2</sub>SO<sub>4</sub> aqueous

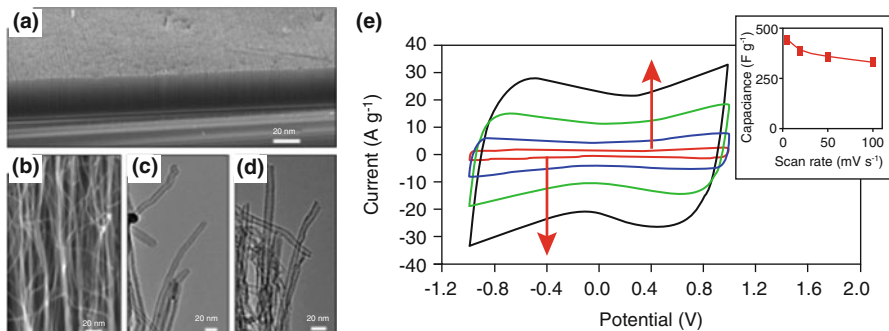


**Fig. 1.7** (a) Low- (b) high-magnification SEM images of vertically-aligned CNTs etched by O<sub>2</sub> plasma. TEM images of the CNTs before (c) and after (d) plasma etching. (e) CV curves of plasma-etched vertically-aligned CNTs as electrode in [EMIM][Tf<sub>2</sub>N] electrolyte at different scan rates. Inset exhibits capacitances as a function of scan rate (Lu et al. 2009)

solution decreased from 113.84° for original MWCNT powders to 36.48° and 19.87° for microwave- and O<sub>2</sub> plasma-treated MWCNTs, respectively (Dulyaseree et al. 2016). This suggests that treated MWCNTs are hydrophilic. The corresponding specific capacitances in 1 M Na<sub>2</sub>SO<sub>4</sub> electrolyte increase from 61.5 F g<sup>-1</sup> for original MWCNT powders to 214 and 238 F g<sup>-1</sup> for microwave- and O<sub>2</sub> plasma-treated MWCNTs, respectively (Dulyaseree et al. 2016). The capacitance improvement is ascribed to the increase in the number of oxygen-containing functional groups. However, plasma activated carbon electrodes decorated with functional groups may potentially have some issues with low cycle stability and high leakage current. Therefore, such research involving plasma activation should be further investigated in the coming days.

Apart from improving the specific surface area, there is another way to increase the specific capacitance by doping CNTs with heteroatoms, which leads to increasing the electrical conductivity and active sites on CNTs. For example, Gueon et al. synthesized N-doped CNT spherical particles by emulsion-assisted evaporation of hexadecane, followed by N-doping using melamine (Gueon and Moon 2015). A specific capacitance of 215 F g<sup>-1</sup> has been obtained at a current density of 0.2 A g<sup>-1</sup>, which is 3.1 times higher than that of the untreated CNTs. The improved performance may be attributed to more active sites and higher electrical conductivity that stem from the N-doping. Xu et al. prepared porous N-doped CNTs from tubular polypyrrole in a N<sub>2</sub> atmosphere, followed by activation of KOH solution. The resulting porous N-doped CNTs provide a high SSA of 1765 m<sup>2</sup> g<sup>-1</sup> with a specific capacitance of 210 F g<sup>-1</sup> at a current density of 0.5 A g<sup>-1</sup>, and have higher specific capacitance (174 A g<sup>-1</sup>) than the self-assembled graphene hydrogen under the same conditions (160 F g<sup>-1</sup> at 1 A g<sup>-1</sup>) (Xu et al. 2013). Moreover, 99% of the initial capacitance was maintained after 5000 cycles. The excellent performance of porous N-doped CNTs can be attributed to high electrical conductivity, large surface area, and unique pore-size distribution (Xu et al. 2013).



Compared to EDLCs, pseudo-capacitors exhibit higher capacitance due to their charge storage mechanism (fast and reversible redox reactions). In order to achieve higher specific capacitance, CNTs have been extensively utilized as pseudo-capacitors in combination with other active components, e.g., conductive polymers, metal oxides and hydroxides. Among them, conducting polymers have some advantages including mass production, environmental friendliness, low weight as well as low-cost. The conducting polymers providing good electrical conductivity, intrinsic porosity, and plenty of redox moieties have demonstrated high specific capacitance when composited with CNTs. At present, most studied conducting polymers are polypyrrole (PPy), polythiophene (PT), polyaniline (PANI), and poly(3,4-ethylenedioxythiophene) (PEDOT) for pseudo-capacitors. Jurewicz et al. deposited a PPy layer of 5 nm on MWCNTs by electrochemical polymerization of pyrrole, and increased the specific capacitance of  $163 \text{ F g}^{-1}$  from the pristine MWCNTs of  $50 \text{ F g}^{-1}$  in a 1 M  $\text{H}_2\text{SO}_4$  electrolyte (Jurewicz et al. 2001). Higher specific capacitance of  $249 \text{ F g}^{-1}$  for PPy/CNT composite electrodes has been realized with CNT content of 81.8 wt% (Li et al. 2014). Xu et al. reported the PPy/CNT sponges have an increase in specific capacitance from 224 to  $350 \text{ F g}^{-1}$  with increasing CNT content from 30 wt% to 49% (Xu et al. 2015). However, with further increasing CNT content to 66 wt%, the capacitance decreased to  $153 \text{ F g}^{-1}$ . This may ascribe to the lower intrinsic capacitance of CNT and smaller contribution from PPy for this pseudo-capacitor (Paul et al. 2010). In comparison with other conducting polymers, PANI has a higher theoretical specific capacitance (Li et al. 2009). Bavio et al. synthesized PANI/CNT composites through a chemical method of self-organization, and investigated the PANI/CNT composites in a 0.5 M  $\text{H}_2\text{SO}_4$  electrolyte (Bavio et al. 2014). The specific capacitance increased to  $838 \text{ F g}^{-1}$  at a current density of  $2 \text{ Ag}^{-1}$  from pristine PANI of  $314 \text{ F g}^{-1}$ , and further increased to  $1744 \text{ F g}^{-1}$  when the embedded CNTs were previously functionalized in 2.2 M  $\text{HNO}_3$ .

Metal oxides and hydroxides including  $\text{Co}_3\text{O}_4$ ,  $\text{Fe}_3\text{O}_4$ , NiO,  $\text{MnO}_2$ ,  $\text{Mn}_3\text{O}_4$ ,  $\text{RuO}_2$ ,  $\text{SnO}_2$ ,  $\text{TiO}_2$ , and  $\text{Ni}(\text{OH})_2$  have also attracted great attention in the field of pseudo-capacitors, in which fast and reversible redox reactions take place on the electrode surfaces. The redox phenomenon of all these oxides involves into the polyvalent nature of the transition metals in the oxidation states. The oxides interact with protons and/or hydroxide anions on changing their oxidation states and the corresponding redox behavior not only exists on the surface of the electrodes but also influences the oxide bulk. Despite their excellent specific capacitance, most of the oxides encountered some issues, e.g. low electrical conductivity (except  $\text{RuO}_2$ ), poor stability, and low rate capability. The carbon materials can not only overcome these disadvantages mentioned above for these oxides, but also restrict the volumetric change of the oxides during the charge-discharge processes. The combination of metal oxides with carbon materials has already demonstrated high performances in pseudo-capacitors.

$\text{MnO}_2$  have a high theoretical specific capacitance of  $1370 \text{ F g}^{-1}$  (Toupin et al. 2004). The  $\text{MnO}_2$ /CNT composites have shown the high specific capacitance between 115 and  $950 \text{ F g}^{-1}$  in pseudo-capacitors (Yan et al. 2009a). As shown in



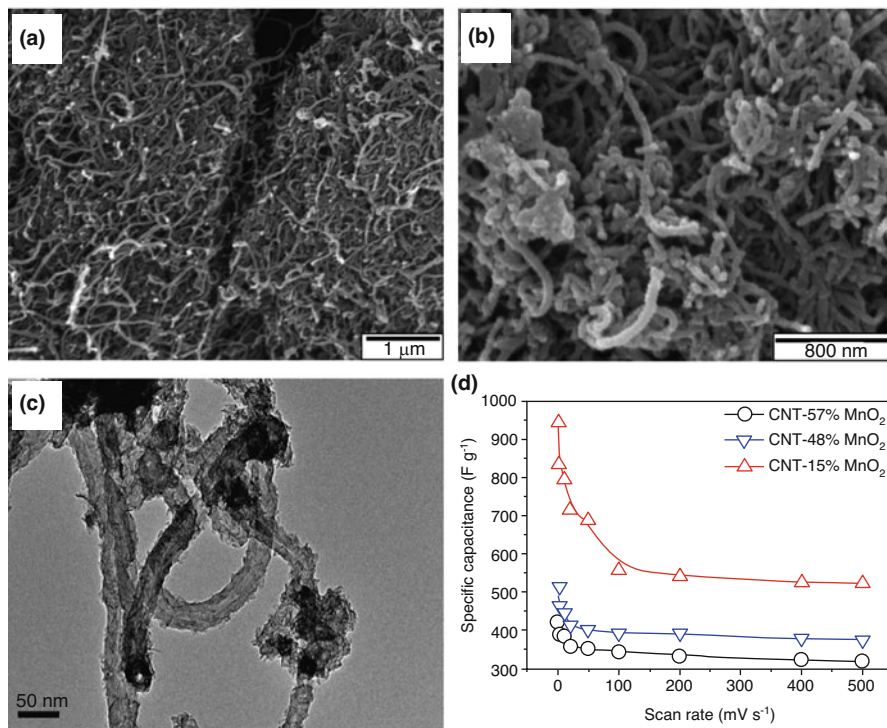


**Fig. 1.8** (a) SEM image of purified CNTs. (b) SEM and (c) TEM images of CNT-57%MnO<sub>2</sub> composite. (d) Specific capacitance of CNT/MnO<sub>2</sub> composites based on MnO<sub>2</sub> at different rates (Yan et al. 2009a)

Fig. 1.8, Yan et al. reported that MnO<sub>2</sub>/CNT composites were synthesized by reduction of KMnO<sub>4</sub> under microwave irradiation, and showed a specific capacitance of 944 F g<sup>-1</sup> at the scan rate of 1 mV s<sup>-1</sup> in 1 M Na<sub>2</sub>SO<sub>4</sub> aqueous solution for the MnO<sub>2</sub>/CNT composites (containing 15 wt% MnO<sub>2</sub>). These supercapacitor electrodes have the maximum power density of 45.4 kW kg<sup>-1</sup> and the energy density of 25.2 Wh kg<sup>-1</sup> when the MnO<sub>2</sub> content is 57 wt%.

As RuO<sub>2</sub> have relatively high conductivity, highly reversible redox reactions, three oxidation states, and wide operation potential window (1.2 V in acidic solutions), RuO<sub>2</sub>/CNT composites as supercapacitor electrodes have been widely studied for pseudo-capacitors with high specific capacitance (Borenstein et al. 2017). Initially, the amorphous or nanoscale crystalline RuO<sub>2</sub>·xH<sub>2</sub>O powders were mixed mechanically with the HNO<sub>3</sub>-treated MWCNTs to fabricate the RuO<sub>2</sub>/CNT composites for supercapacitor electrodes (Ma et al. 2000). Depending on the weight content of RuO<sub>2</sub>·xH<sub>2</sub>O, the composites have reached the specific capacitance of 145–560 F g<sup>-1</sup> in a 38% H<sub>2</sub>SO<sub>4</sub> solution. Yan et al. also synthesized RuO<sub>2</sub> nanoparticles on MWCNTs by microwave-assisted irradiation for supercapacitor electrodes, and displayed high specific capacitance up to 493.9 F g<sup>-1</sup> at the scan rate

of  $50 \text{ mV s}^{-1}$  in  $1 \text{ M H}_2\text{SO}_4$  aqueous solution (Yan et al. 2009b). Most of investigations have demonstrated that the  $\text{RuO}_2/\text{CNT}$  composites have high energy densities at high power densities, and exhibit excellent cycling stability.

### 1.4.2 Graphene in Electrochemical Capacitors

Graphene, consisting of carbon atoms arranged in a hexagonal network, has been considered an electrode candidate for ECs due to high carrier mobility, excellent mechanical properties, chemical stability, and high surface area. The theoretical specific surface area of graphene was predicted to be  $2630 \text{ m}^2 \text{ g}^{-1}$ , which can produce high specific capacitance of  $550 \text{ F g}^{-1}$  (El-Kady et al. 2012). A pioneer work employing chemically-modified graphene (reduced graphene oxide, rGO) as supercapacitor electrodes had exhibited a specific capacitance of  $137 \text{ F g}^{-1}$  with a SSA of  $705 \text{ m}^2 \text{ g}^{-1}$  in a  $5.5 \text{ M KOH}$  electrolyte (Stoller et al. 2008), which is lower than the theoretic SSA of  $2630 \text{ m}^2 \text{ g}^{-1}$ , possibly due to the aggregation of rGO. In order to improve the SSA, Zhu et al. (2011) utilized chemical activation process to activate exfoliated GO with KOH, and obtained a very high SSA of  $3100 \text{ m}^2 \text{ g}^{-1}$ , which is even higher than the theoretic value and ascribed to the presence of 3D structure containing pores with sizes of  $1\text{--}10 \text{ nm}$  (Fig. 1.9a, b). Figure 1.9c, d shows that the authors assembled the two-electrode symmetrical supercapacitors based on the activated GO in 1-butyl-3-methyl-imidazolium tetrafluoroborate (BMIM  $\text{BF}_4$ )/AN electrolyte, and obtained the specific capacitance from the galvanostatic charge/

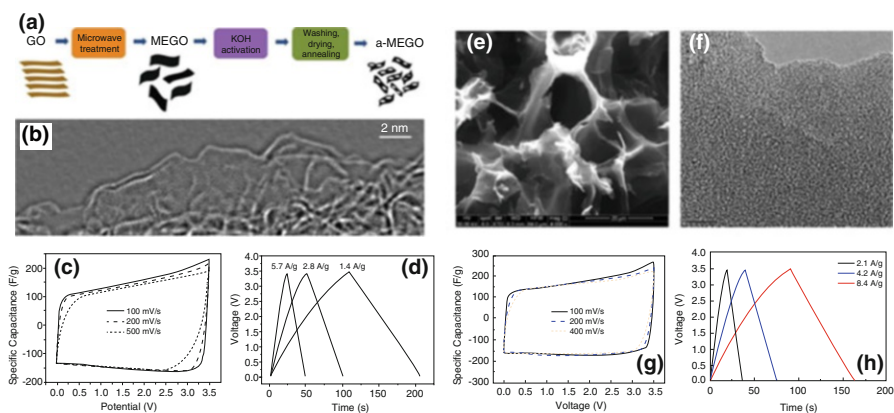


**Fig. 1.9** (a) Schematic diagram displaying the microwave exfoliation/reduction of GO and the following chemical activation of MEGO with KOH. (b) High-resolution TEM image from the edge of a-MEGO. (c) CV curves of the a-MEGO-based supercapacitor at different scan rates. (d) The corresponding Galvanostatic charge/discharge under different constant currents. (e) SEM and (f) TEM images of activated hollow spheres of microwave-expanded GO (asMEGO). (g) CV curves of asMEGO at different scan rates. (h) The corresponding Galvanostatic charge/discharge under different constant currents (Zhu et al. 2011; Kim et al. 2013)

discharge curve with values of 165, 166, and 166 F g<sup>-1</sup> at the current densities of 1.4, 2.8, and 5.7 A g<sup>-1</sup>, respectively (Zhu et al. 2011). In another work, as shown in Fig. 1.9e–h, the same group further improved the SSA to 3290 m<sup>2</sup> g<sup>-1</sup> for highly porous graphene, which derived from carbons with hierarchical pore structures consisting of mesopores integrated with macroporous scaffolds, and exhibited a specific capacitance of 174 F g<sup>-1</sup> with energy density and power density of 74 Wh kg<sup>-1</sup> and 338 kW kg<sup>-1</sup>, respectively (Kim et al. 2013).

Like doped CNTs, heteroatom-doped graphene has better performance in the application of energy storage compared to pristine graphene, ascribing to the improved electrical and electrochemical properties. Jeong et al. synthesized nitrogen-doped graphene by a nitrogen plasma process from GO, and obtained a specific capacitance of 282 F g<sup>-1</sup> for N-doped graphene, which is four times than that of pristine graphene (Jeong et al. 2011). This is attributed to the introduction of charge-transferring sites stemming from N-doping and improvement of electrical conductivity of graphene. Moreover, a power density of  $8 \times 10^5$  W kg<sup>-1</sup> and an energy density of 48 Wh kg<sup>-1</sup> were achieved in the organic electrolyte of TEA BF<sub>4</sub>. Besides N-doping, other elements including boron, sulfur, phosphorous and their co-doping have been employed to improve the specific capacitance of graphene (Han et al. 2012; Chen et al. 2014; Karthika et al. 2013; Wang et al. 2014b).

Graphene has also been investigated with other active materials, e.g., conducting polymers, metal oxides and hydroxides, to form composites as electrodes for pseudo-capacitors. Firstly, freestanding and flexible GO/PANI composite paper was prepared by in-situ anodic electropolymerization of PANI film on GO paper, and exhibited the gravimetric and volumetric capacitances of 233 F g<sup>-1</sup> and 135 F cm<sup>-3</sup> in the electrolyte of 1 M H<sub>2</sub>SO<sub>4</sub>, respectively, much higher than those of the GO paper (Wang et al. 2009). Zhang et al. employed in-situ polymerization of aniline monomer in the GO surface to fabricate graphene/PANI nanofiber composites under acid conditions, and achieved a specific capacitance of 480 F g<sup>-1</sup> at a current density of 0.1 A g<sup>-1</sup> in a 2 M H<sub>2</sub>SO<sub>4</sub> for a PANI-doped graphene composite (Zhang et al. 2010). The results showed that the specific capacitance of PANI/GO electrodes is very strongly dependent of the mass ratio of PANI to GO. Besides PANI, PPy has also been composited with graphene to synthesize PPy/GO films by electrooxidation of pyrrole in the GO aqueous solution, which were further reduced electrochemically to form PPy/rGO composites (Chang et al. 2012), as shown in Fig. 1.10. These PPy/rGO composite films exhibited a specific capacitance of 424 F g<sup>-1</sup> in 1 M H<sub>2</sub>SO<sub>4</sub> at a current density of 1 A g<sup>-1</sup>, which was higher than those of a surfactant-intercalated GO (194 F g<sup>-1</sup>) (Zhang et al. 2011), resorcinol-formaldehyde resin/GO composite (316 F g<sup>-1</sup>) (Rightmire 1966), and a PANI nanofiber/GO composite (210 F g<sup>-1</sup>) (Zhang et al. 2010). The high specific capacitance for the PPy/rGO composite ascribed to the fast insertion/extraction of doping ions in PPy/rGO matrix, high conductivity and high effective SSA of the composite films.

Similar to the case for CNTs, metal oxides or hydroxides have also been investigated in the graphene-based composites to improve the pseudocapacitance. Graphene was used for loading MnO<sub>2</sub> to form composite electrodes with high

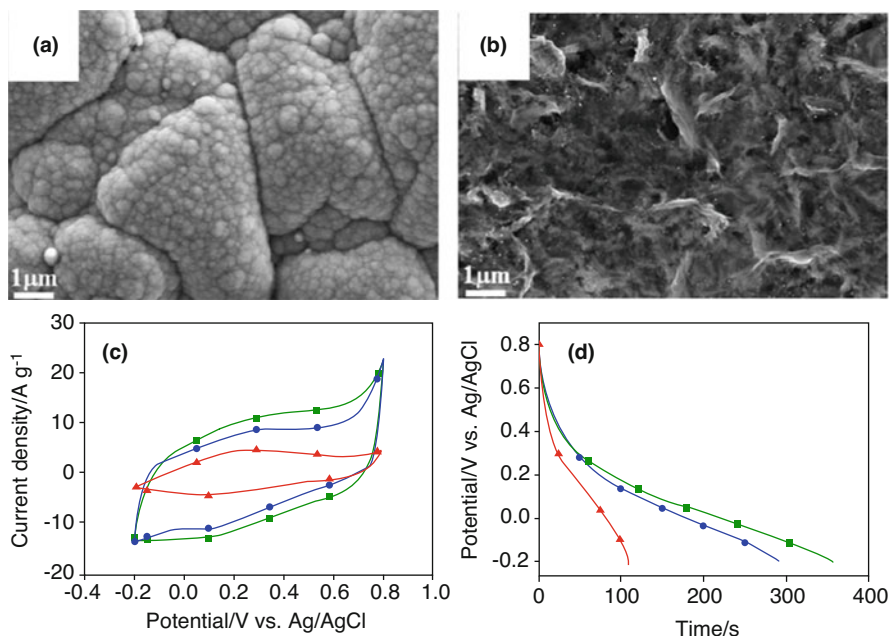


**Fig. 1.10** SEM images of (a) PPy film and (b) PPy/GO composite film coated on gold electrode. The films were synthesized by passing  $130 \text{ mC cm}^{-2}$  of charge at  $+0.8 \text{ V}$  vs. Ag/AgCl. (c) CV curves of PPy (red triangle), PPy/GO (blue dot), and PPy/rGO (green square) modified gold electrodes in  $1 \text{ M H}_2\text{SO}_4$  at  $0.1 \text{ V s}^{-1}$ . (d) Galvanostatic discharge/charge curves of PPy (red triangle), PPy/GO (blue dot), and PPy/rGO (green square) modified gold electrodes in  $1 \text{ M H}_2\text{SO}_4$  at a current density of  $1 \text{ A g}^{-1}$  (Chang et al. 2012)

conductivity, large surface area, and excellent stability. The  $\text{MnO}_2/\text{graphene}$  composites have demonstrated high specific capacitance in the range of  $300\text{--}520 \text{ F g}^{-1}$  (Yan et al. 2010). Yan et al. synthesized  $\text{MnO}_2/\text{graphene}$  composites by the self-limiting deposition of nanoscale  $\text{MnO}_2$  on the GO surface under microwave irradiation, and presented a specific capacitance as high as  $310 \text{ F g}^{-1}$  and  $228 \text{ F g}^{-1}$  in  $1 \text{ M Na}_2\text{SO}_4$  electrolyte at the scan rates of  $2 \text{ mV s}^{-1}$  and  $500 \text{ mV s}^{-1}$ , respectively, which are higher than these of pure graphene ( $104 \text{ F g}^{-1}$ ) and birnessite-type  $\text{MnO}_2$  ( $103 \text{ F g}^{-1}$ ). Moreover, these composites displayed excellent cycling stability and a decrease of 4.6% in the initial capacity after 15,000 cycles. These excellent electrochemical performances can be attributed to the increased conductivity and surface area of graphene network in the  $\text{MnO}_2/\text{graphene}$  composites. Alternatively, Cheng et al. electrodeposited gamma-type  $\text{MnO}_2$  on the graphene surface to increase the specific capacitance of  $328 \text{ F g}^{-1}$  of the  $\text{MnO}_2/\text{graphene}$  composites from  $245 \text{ F g}^{-1}$  of pure graphene electrode in  $1 \text{ M KCl}$  at a charging current of  $1 \text{ mA}$  (Cheng et al. 2011). The  $\text{MnO}_2/\text{graphene}$  composites also demonstrated an energy density of  $11.4 \text{ Wh kg}^{-1}$  and a power density of  $25.8 \text{ kW kg}^{-1}$ , respectively.

Besides flat graphene related to substrate, vertical graphene (VG) is another type of graphene, consists of a large amount of edges with open structures, and has some advantages compared to flat graphene as follows (Miller et al. 2010): (1) VGs can provide direct pathways for ion faster diffusion; (2) edge planes have higher capacitance of 50–70  $\mu\text{F cm}^{-1}$  in comparison to basal planes of about 3  $\mu\text{F cm}^{-1}$ ; (3) open structures lead to minimal porosity effects, and reduce ionic resistance; (4) VG (using plasma technique) can grow on the conducting substrates, and be used as electrode without binder to minimize electronic resistances. The VG, which grew on carbon fibers by radio frequency plasma-enhanced chemical vapor deposition in  $\text{H}_2\text{-CH}_4$  system, have the specific capacitance of 0.076  $\text{F cm}^{-2}$  and a value of 14,900 F at maximum working voltage of 0.6 V in 6 M  $\text{H}_2\text{SO}_4$  electrolyte (Zhao et al. 2009). The EDLCs made of VG, which deposited directly on the Ni foil from the decomposition of  $\text{CH}_4$ , have demonstrated fast response with efficient line-filtering at 120 Hz (Miller et al. 2010). It ascribes to the open morphology of VG that provides high conductance channels for ingress and egress of the electrolyte ions between the vertical sheets, which minimize porous electrode behavior and allow fast response. The specific capacitance of the EDLCs can be improved using the feedstock of  $\text{C}_2\text{H}_2$  instead of  $\text{CH}_4$  or increasing the VG growth temperatures (Cai et al. 2014), as shown in Fig. 1.11.

For graphene-based electrode materials, N-doping is one of the popular methods for enhancing the performance of supercapacitors. For example, Yen et al. synthesized N-doped VG on flexible carbon cloths by microwave PECVD, where followed by introducing in situ  $\text{NH}_3$  plasma (Yen et al. 2015). The resulting N-doped VG supercapacitor electrodes exhibited a specific capacitance of 991.6  $\text{F g}^{-1}$  at a current density of 14.8  $\text{A g}^{-1}$ , obtained the highest specific energy density of 275.4  $\text{Wh kg}^{-1}$  a power density of 14.8  $\text{kW kg}^{-1}$ , and maintained near 98% Coulombic efficiency after 5000 cycles at in 1 M  $\text{H}_2\text{SO}_4$  aqueous solution (Yen et al. 2015). These excellent performances attributed to the ultrahigh surface area of VG and unique specificity to the pyridinic N-doping configuration (Yen et al. 2015). The VG can also provide a support for loading metal oxides or hydroxides on its surface in the applications of pseudo-capacitors (Xiong et al. 2013; Hassan et al. 2014a, b; Wang et al. 2014a; Dinh et al. 2014; Han et al. 2017). Xiong et al. reported that VG was prepared by microwave PECVD on commercial CNT substrates and subsequently coated with a thin layer of  $\text{MnO}_2$ , and investigated the electrochemical performances of the  $\text{MnO}_2/\text{VG}$  composites (Xiong et al. 2013). A specific capacitance of 580  $\text{F g}^{-1}$  at a scan rate of 2  $\text{mV s}^{-1}$ , and an energy density of 28  $\text{Wh kg}^{-1}$  and a power density of 25  $\text{kW kg}^{-1}$  at a high current density of 50  $\text{A g}^{-1}$  have been achieved in 1 M  $\text{Na}_2\text{SO}_4$  aqueous electrolyte (Xiong et al. 2013). This good performance could be obtained due to the VG/CNT architecture without binder and the metallic nature of  $\text{MnO}_2/\text{VG}$  composites with a facile conduction path for electron transport in the charge/discharge process (Xiong et al. 2013).

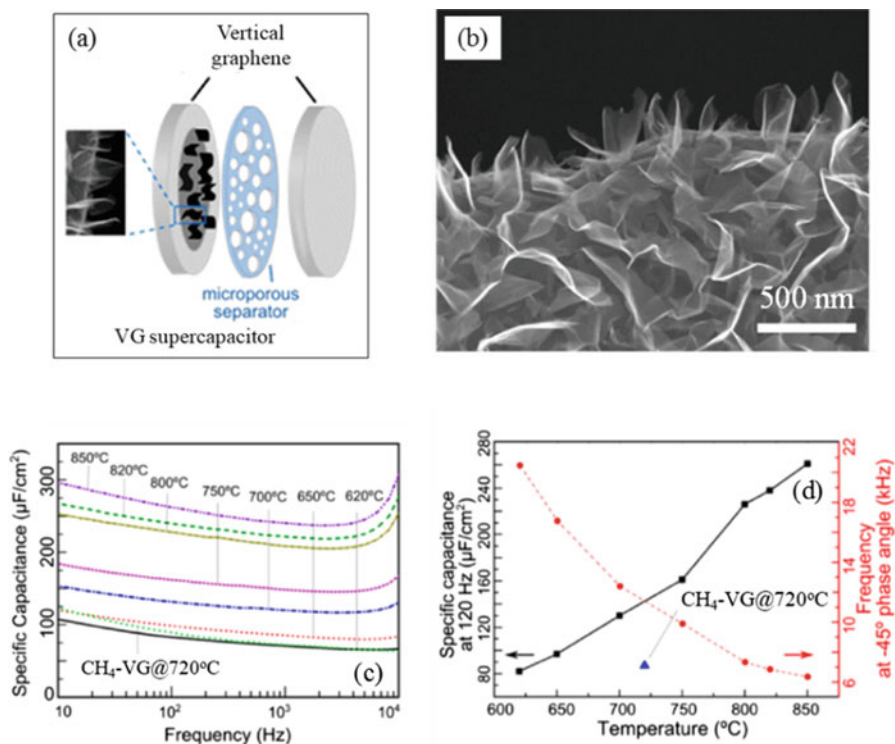


**Fig. 1.11** (a) Schematic diagram of VG supercapacitor which consists of two same VG sheets. (b) SEM images of VG sheets. (c) Specific capacitance of EDLCs, which consist of C<sub>2</sub>H<sub>2</sub>-VG at different temperatures, as a function of frequency. The higher the growth temperature, the higher the capacitance over the entire frequency range for all samples. (d) The specific capacitance of EDLCs at 120 Hz (black square blocks) for 10 min growth and the characteristic frequency  $f_0$  (red circular dots) as a function of growth temperature. The EDLC made of CH<sub>4</sub>-VG@720 °C as a comparison (Cai et al. 2014)

## 1.5 Future Perspectives, Opportunities, and Challenges

In comparison with batteries, it is undeniable that even though supercapacitors offer higher power, relatively good cycle life, and higher reliability, they exhibited much lower energy density and higher self-discharge (Weinstein and Dash 2013). Nevertheless, some supercapacitors have been applied for emergency doors, memory backup, and energy recovery, despite the fact that limited energy density still remain as the big challenge.

Carbon materials derived from waste materials such as agricultural wastes, especially coconut shell ACs can be considered as the popular option for active material (Weinstein and Dash 2013). Kuraray (Japan) is one of the major suppliers for most of this product. One of the main reasons is that coconut shell ACs offers far more lower cost, in contrast to another types of carbon materials.



Carbon nanomaterials such as CNTs and graphene have received much attention, to be developed as high performance supercapacitor electrode material. For the time being, although their costs are higher than AC, they are able to close the performance gap, which is essential so that supercapacitor can be applied for wide broad applications in various fields. In addition to electrode materials, electrolyte also plays a crucial role in determining the performance outcome of supercapacitors. It is known that energy storage density is proportional to the square of the operating voltage, thus using alternative electrolyte systems with significantly wider operating voltage stability windows can significantly improve the energy storage capability of supercapacitors (Yu et al. 2013). Future advancement of supercapacitors can be shifted to develop appropriate morphology and porous structure of carbon nanomaterials that have high compatibility with the improved electrolyte, development of novel nanostructured metal oxides/conductive polymers to improve energy storage capabilities, development of computational tools to investigate the mechanisms during charge/discharge process, and so on.

## 1.6 Conclusions

In this chapter, energy storage performance of electrochemical capacitors or supercapacitors was discussed focusing on carbon nanomaterials, specifically CNTs, graphene, and their derivatives. The affecting factors of two main elements, namely electrode and electrolyte materials were elaborated, which is highly associated with the overall supercapacitor's performance. Various types of materials utilized together with carbon nanomaterials, such as metal oxides, conductive polymers, doped materials, and so on, were also included. The development of safe, low cost, high energy storage, fast charge/discharge process, long cycle life supercapacitors is essential in order to produce efficient energy storage device.

## References

- Abioye AM, Noorden ZA, Ani FN (2017) Synthesis and characterizations of electroless oil palm shell based-activated carbon/nickel oxide nanocomposite electrodes for supercapacitor applications. *Electrochim Acta* 225:493–502. <https://doi.org/10.1016/j.electacta.2016.12.101>
- An KH, Kim WS, Park YS, Moon J-M, Bae DJ, Lim SC, Lee YS, Lee YH (2001) Electrochemical properties of high-power supercapacitors using single-walled carbon nanotube electrodes. *Adv Funct Mater* 11(5):387–392. <https://doi.org/10.1002/1616-301X/01/0510-0387>
- Barbieri O, Hahn M, Herzog A, Kotz R (2005) Capacitance limits of high surface area activated carbons for double layer capacitors. *Carbon* 43:1303–1310. <https://doi.org/10.1016/j.carbon.2005.01.001>
- Bavio MA, Acosta GG, Kessler T (2014) Synthesis and characterization of polyaniline and polyaniline-carbon nanotubes nanostructures for electrochemical supercapacitors. *J Power Sources* 245:475–481. <https://doi.org/10.1016/j.jpowsour.2013.06.119>
- Becker H I (1957) Low voltage electrolytic capacitor. US Patent 2800616

- Bichat MP, Raymundo-Piñero E, Béguin F (2010) High voltage supercapacitor built with seaweed carbons in neutral aqueous electrolyte. *Carbon* 48(15):4351–4361. <https://doi.org/10.1016/j.carbon.2010.07.049>
- Boos D L (1970) Electrolytic capacitor having carbon paste electrodes. US Patent 3536963
- Borenstein A, Hanna O, Attias R, Luski S, Brousse T, Aurbach D (2017) Carbon-based composite materials for supercapacitor electrode: a review. *J Mater Chem A* 5(25):12653–12672. <https://doi.org/10.1039/c7ta00863e>
- Cai M, Outlaw RA, Quinlan RA, Premathilake D, Butler SM, Miller JR (2014) Fast response, vertically oriented graphene nanosheet electric double layer capacitors synthesized from C<sub>2</sub>H<sub>2</sub>. *ACS Nano* 8(6):5873–5882. <https://doi.org/10.1021/nn5009319>
- Chang H-H, Chang C-K, Tsai Y-C, Liao C-S (2012) Electrochemically synthesized graphene/polypyrrole composites and their use in supercapacitor. *Carbon* 50(6):2331–2336. <https://doi.org/10.1016/j.carbon.2012.01.056>
- Chen T, Dai L (2013) Carbon nanomaterials for high-performance supercapacitors. *Mater Today* 16(7-8):272–280. <https://doi.org/10.1016/j.mattod.2013.07.002>
- Chen X, Chen X, Xu X, Yang Z, Liu Z, Zhang L, Xu X, Chen Y, Huang S (2014) Sulfur-doped porous reduced graphene oxide hollow nanosphere frameworks as metal-free electrocatalysts for oxygen reduction reaction and as supercapacitor electrode materials. *Nanoscale* 6(22):13740–13747. <https://doi.org/10.1039/C4NR04783D>
- Cheng Q, Tang J, Ma J, Zhang H, Shinya N, Qin L-C (2011) Graphene and nanostructured MnO<sub>2</sub> composite electrodes for supercapacitors. *Carbon* 49(9):2917–2925. <https://doi.org/10.1016/j.carbon.2011.02.068>
- Chmiola J, Yushin G, Dash R, Gogotsi Y (2006a) Effect of pore size and surface area of carbide derived carbons on specific capacitance. *J Power Sources* 158(1):765–772. <https://doi.org/10.1016/j.jpowsour.2005.09.008>
- Chmiola J, Yushin G, Gogotsi Y, Portet C, Simon P, Taberna PL (2006b) Anomalous increase in carbon capacitance at pore sizes less than 1 nanometer. *Science* 313(5794):1760–1763. <https://doi.org/10.1126/science.1132195>
- Conway BE (1999) *Electrochemical supercapacitors: scientific fundamentals and technological applications*. Kluwer Academic/Plenum Publishers, New York, NY
- Dai L, Chang DW, Baek J-B, Lu W (2012) Carbon nanomaterials for advanced energy conversion and storage. *Small* 8(8):1130–1166. <https://doi.org/10.1002/smll.201101594>
- Dinh TM, Achour A, Vizireanu S, Dinescu G, Nistor L, Armstrong K, Guay D, Pech D (2014) Hydrous RuO<sub>2</sub>/carbon nanowalls hierarchical structures for all-solid-state ultrahigh-energy-density micro-supercapacitors. *Nano Energy* 10:288–294. <https://doi.org/10.1016/j.nanoen.2014.10.003>
- Dong Y, Wu Z-S, Ren W, Cheng HM, Bao X (2017) Graphene: a promising 2D material for electrochemical energy storage. *Sci Bull* 62(10):724–740. <https://doi.org/10.1016/j.scib.2017.04.010>
- Dulyaseree P, Yordsri V, Wongwiriyan W (2016) Effects of microwave and oxygen plasma treatments on capacitive characteristics of supercapacitor based on multiwalled carbon nanotubes. *Jpn J Appl Phys* 55:02BD05. <https://doi.org/10.7567/JJAP.55.02BD05>
- El-Kady MF, Strong V, Dubin S, Kaner RB (2012) Laser scribing of high-performance and flexible graphene-based electrochemical capacitors. *Science* 335(6074):1326–1330. <https://doi.org/10.1126/science.1216744>
- Fauvarque JF, Simon P (2010) Principles of electrochemistry and electrochemical methods. In: Béguin F, Frackowiak E (eds) *Carbons for electrochemical energy storage and conversion systems*. CRC Press, Boca Raton, pp 1–36
- Frackowiak E, Béguin F (2001) Carbon materials for the electrochemical storage of energy in capacitors. *Carbon* 39(6):937–950. [https://doi.org/10.1016/S0008-6223\(00\)00183-4](https://doi.org/10.1016/S0008-6223(00)00183-4)
- Frackowiak E, Metenier K, Bertagna V, Béguin F (2000) Supercapacitor electrodes from multiwalled carbon nanotubes. *Appl Phys Lett* 77:2421–2423. <https://doi.org/10.1063/1.1290146>



- Frackowiak E, Delpoux S, Jurewicz K, Szostak K, Cazorla-Amoros D, Beguin F (2002) Enhanced capacitance of carbon nanotubes through chemical activation. *Chem Phys Lett* 361(1–2):35–41. [https://doi.org/10.1016/S0009-2614\(02\)00684-X](https://doi.org/10.1016/S0009-2614(02)00684-X)
- Futaba DN, Hata K, Yamada T, Hiraoka T, Hayamizu Y, Kakudate Y, Tanaike O, Hatori H, Yumura M, Iijima S (2006) Shape-engineerable and highly densely packed single-walled carbon nanotubes and their application as super-capacitor electrodes. *Nat Mater* 5(12):987–994. <https://doi.org/10.1038/nmat1782>
- Gu W, Yushin G (2014) Review of nanostructured carbon materials for electrochemical capacitor applications: advantages and limitations of activated carbon, carbide-derived carbon, zeolite-templated carbon, carbon aerogels, carbon nanotubes, onion-like carbon and graphene. *WIREs Energy Environ* 3(5):424–473. <https://doi.org/10.1002/wene.102>
- Gueon D, Moon JH (2015) Nitrogen-doped carbon nanotube spherical particles for supercapacitor applications: emulsion-assisted compact packing and capacitance enhancement. *ACS Appl Mater Interfaces* 7(36):20083–20089. <https://doi.org/10.1021/acsami.5b05231>
- Han J, Zhang LL, Lee S, Oh J, Lee K-S, Potts JR, Ji J, Zhao X, Ruoff RS, Park S (2012) Generation of B-doped graphene nanoplatelets using a solution process and their supercapacitor applications. *ACS Nano* 7(1):19–26. <https://doi.org/10.1021/nm3034309>
- Han ZJ, Pineda S, Murdock AT, Seo DH, Ostrikov K, Bendavid A (2017) RuO<sub>2</sub>-coated vertical graphene hybrid electrodes for high-performance solid-state supercapacitors. *J Mater Chem A* 5(33):17293–17301. <https://doi.org/10.1039/C7TA03355A>
- Hassan S, Suzuki M, Mori S, El-Moneim AA (2014a) MnO<sub>2</sub>/carbon nanowalls composite electrode for supercapacitor applications. *J Power Sources* 249:21–27. <https://doi.org/10.1016/j.jpowsour.2013.10.097>
- Hassan S, Suzuki M, Mori S, El-Moneim AA (2014b) MnO<sub>2</sub>/carbon nanowall electrode for future energy storage application: effect of carbon nanowall growth period and MnO<sub>2</sub> mass loading. *RSC Adv* 4(39):20479–20488. <https://doi.org/10.1039/c4ra01132e>
- He N, Yildiz O, Pan Q, Zhu J, Zhang X, Bradford PD, Gao W (2017) Pyrolytic-carbon coating in carbon nanotube foams for better performance in supercapacitors. *J Power Sources* 343:492–501. <https://doi.org/10.1016/j.jpowsour.2017.01.091>
- Hierold C, Brand O, Fedder GK, Korvink JG, Tabata O (2008) Carbon nanotube devices: properties, modeling, integration and applications, vol 8. John Wiley & Sons, Chichester
- Hsu Y-K, Chen Y-C, Lin Y-G, Chen L-C, Chen K-H (2012) High-cell-voltage supercapacitor of carbon nanotube/carbon cloth operating in neutral aqueous solution. *J Mater Chem* 22(8):3383–3387. <https://doi.org/10.1039/C1JM14716A>
- Hu L, Hecht DS, Gruner G (2010) Carbon nanotube thin films: fabrication, properties, and applications. *Chem Rev* 110(10):5790–5844. <https://doi.org/10.1021/cr9002962>
- Huang Y, Liu Y, Zhao G, Chen JY (2017) Sustainable activated carbon fiber from sawdust by reactivation for high-performance supercapacitors. *J Mater Sci* 52(1):478–488. <https://doi.org/10.1007/s10853-016-0347-0>
- Iijima S (1991) Helical microtubules of graphitic carbon. *Nature* 354(6348):56–58. <https://doi.org/10.1038/354056a0>
- Iijima S, Ichihashi T (1993) Single-shell carbon nanotubes of 1-nm diameter. *Nature* 363(6430):603–605. <https://doi.org/10.1038/363603a0>
- Jeong HM, Lee JW, Shin WH, Choi YJ, Shin HJ, Kang JK, Choi JW (2011) Nitrogen-doped graphene for high-performance ultracapacitors and the importance of nitrogen-doped sites at basal planes. *Nano Lett* 11(6):2472–2477. <https://doi.org/10.1021/nl2009058>
- Jiang Q, Qu MZ, Zhou GM, Zhang BL, Yu ZL (2002) A study of activated carbon nanotubes as electrochemical super capacitors electrode materials. *Mater Lett* 57(4):988–991. [https://doi.org/10.1016/S0167-577X\(02\)00911-4](https://doi.org/10.1016/S0167-577X(02)00911-4)
- Jo EH, Jang HD, Chang H, Kim SK, Choi J-H, Lee CM (2017) 3D network-structured crumpled graphene/carbon nanotube/polyaniline composites for supercapacitors. *ChemSusChem* 10(10):2210–2217. <https://doi.org/10.1002/cssc.201700212>

- Jurewicz K, Delpoux S, Bertagna V, Beguin F, Frackowiak E (2001) Supercapacitors from nanotubes/polypyrrole composites. *Chem Phys Lett* 347(1–3):36–40. [https://doi.org/10.1016/S0009-2614\(01\)01037-5](https://doi.org/10.1016/S0009-2614(01)01037-5)
- Karthika P, Rajalakshmi N, Dhathathreyan KS (2013) Phosphorus-doped exfoliated graphene for supercapacitor electrodes. *J Nanosci Nanotechnol* 13(3):1746–1751. <https://doi.org/10.1166/jnn.2013.7112>
- Ke Q, Wang J (2016) Graphene-based materials for supercapacitor electrodes—a review. *J Mater* 2(1):37–54. <https://doi.org/10.1016/j.jmat.2016.01.001>
- Kim YJ, Yang C-M, Park KC, Kaneko K, Kim YA, Noguchi M, Fujino T, Oyama S, Endo M (2012) Edge-enriched, porous carbon-based, high energy density supercapacitors for hybrid electric vehicles. *ChemSusChem* 5(3):535–541. <https://doi.org/10.1002/cssc.201100511>
- Kim T, Jung G, Yoo S, Suh KS, Ruoff RS (2013) Activated graphene-based carbons as supercapacitor electrodes with macro- and mesopores. *ACS Nano* 7(8):6899–6905. <https://doi.org/10.1021/nn402077v>
- Kroto HW, Heath JR, O'Brien SC, Curl RF, Smalley RE (1985) C<sub>60</sub>: Buckminsterfullerene. *Nature* 318(6042):162–163. <https://doi.org/10.1038/318162a0>
- Largeot C, Portet C, Chmiola J, Taberna P-L, Gogotsi Y, Simon P (2008) Relation between the ion size and pore size for an electric double-layer capacitor. *J Am Chem Soc* 130(9):2730–2731. <https://doi.org/10.1021/ja7106178>
- Li H, Wang J, Chu Q, Wang Z, Zhang F, Wang S (2009) Theoretical and experimental specific capacitance of polyaniline in sulfuric acid. *J Power Sources* 190(2):578–586. <https://doi.org/10.1016/j.jpowsour.2009.01.052>
- Li P, Shi E, Yang Y, Shang Y, Peng Q, Wu S, Wei J, Wang K, Zhu H, Yuan Q (2014) Carbon nanotube-polypyrrole core-shell sponge and its application as highly compressible supercapacitor electrode. *Nano Res* 7(2):209–218. <https://doi.org/10.1007/s12274-013-0388-5>
- Lin T, Chen I-W, Liu F, Yang C, Bi H, Xu F, Huang F (2015) Nitrogen-doped mesoporous carbon of extraordinary capacitance for electrochemical energy storage. *Science* 350(6267):1508–1513. <https://doi.org/10.1126/science.aab3798>
- Lu W, Qu L, Henry K, Dai L (2009) High performance electrochemical capacitors from aligned carbon nanotube electrodes and ionic liquid electrolytes. *J Power Sources* 189(2):1270–1277. <https://doi.org/10.1016/j.jpowsour.2009.01.009>
- Lu Y, Zhang S, Yin J, Bai C, Zhang J, Li Y, Yang Y, Ge Z, Zhang M, Wei L, Ma M, Ma Y, Chen Y (2017) Mesoporous activated carbon materials with ultrahigh mesopore volume and effective specific surface area for high performance supercapacitors. *Carbon* 124:64–71. <https://doi.org/10.1016/j.carbon.2017.08.044>
- Lv W, Li Z, Deng Y, Yang Q-H, Kang F (2016) Graphene-based materials for electrochemical energy storage devices: opportunities and challenges. *Energy Storage Mater* 2:107–138. <https://doi.org/10.1016/j.ensm.2015.10.002>
- Ma R, Wei B, Xu C, Liang J, Wu D (2000) The development of carbon nanotubes/ RuO<sub>2</sub>·xH<sub>2</sub>O electrodes for electrochemical capacitors. *Bull Chem Soc Jpn* 73(8):1813–1816. <https://doi.org/10.1246/bcsj.73.1813>
- Melvin GJH, Wang Z, Siambun NJ, Rahman MM (2017a) Carbon materials derived from rice husks at low and high temperatures. *IOP Conf Ser Mater Sci Eng* 217:012017. <https://doi.org/10.1088/1757-899X/217/1/012017>
- Melvin GJH, Wang Z, Ni QQ, Siambun NJ, Rahman MM (2017b) Fabrication and characterization of carbonized rice husk/barium titanate nanocomposites. *IOP Conf Ser Mater Sci Eng* 229:012024. <https://doi.org/10.1088/1757-899X/229/1/012024>
- Miller JR, Outlaw RA, Holloway BC (2010) Graphene double-layer capacitor with ac-line filtering performance. *Science* 329(5999):1637–1639. <https://doi.org/10.1126/science.1194372>
- Muramatsu H, Kim YA, Yang K-S, Cruz-Silva R, Toda I, Yamada T, Terrones M, Endo M, Hayashi T, Saitoh H (2014) Rice husk-derived graphene with nano-sized domains and clean edges. *Small* 10(14):2766–2770. <https://doi.org/10.1002/smll.201400017>

- Niu C, Sichel EK, Hoch R, Moy D, Tennent H (1997) High power electrochemical capacitors based on carbon nanotube electrodes. *Appl Phys Lett* 70:1480–1482. <https://doi.org/10.1063/1.118568>
- Novoselov KS, Geim AK, Morozov SV, Jiang D, Zhang Y, Dubonos SV, Grigorieva IV, Firsov AA (2004) Electric field effect in atomically thin carbon films. *Science* 306(5696):666–669. <https://doi.org/10.1126/science.1102896>
- Oberlin A, Endo M, Koyama T (1976) Filamentous growth of carbon through benzene decomposition. *J Cryst Growth* 32(3):335–349. [https://doi.org/10.1016/0022-0248\(76\)90115-9](https://doi.org/10.1016/0022-0248(76)90115-9)
- Paul S, Lee Y-S, Choi J-A, Kang Y-C, Kim D-W (2010) Synthesis and electrochemical characterization of polypyrrole/multiwalled carbon nanotube composite electrodes for supercapacitor applications. *Bull Kor Chem Soc* 31(5):1228–1232. <https://doi.org/10.5012/bkcs.2010.31.5.1228>
- Popov VN (2004) Carbon nanotubes: properties and application. *Mater Sci Eng R* 43(3):61–102. <https://doi.org/10.1016/j.mser.2003.10.001>
- Pumera M (2010) Graphene-based nanomaterials and their electrochemistry. *Chem Soc Rev* 39(11):4146–4157. <https://doi.org/10.1039/c002690p>
- Pumera M (2011) Graphene-based nanomaterials for energy storage. *Energy Environ Sci* 4(3):668–674. <https://doi.org/10.1039/C0EE00295J>
- Raymundo-Piñero E, Leroux F, Béguin F (2006) A high-performance carbon for supercapacitors obtained by carbonization of a seaweed biopolymer. *Adv Mater* 18(14):1877–1882. <https://doi.org/10.1002/adma.200501905>
- Rightmire R A (1966) Electrical energy storage apparatus. US Patent 3288641
- Segalini J, Iwama E, Taberna P-L, Gogotsi Y, Simon P (2012) Steric effects in adsorption of ions from mixed electrolytes into microporous carbon. *Electrochem Commun* 15(1):63–65. <https://doi.org/10.1016/j.elecom.2011.11.023>
- Sharma P, Bhatti TS (2010) A review on electrochemical double-layer capacitors. *Energy Convers Manag* 51(12):2901–2912. <https://doi.org/10.1016/j.enconman.2010.06.031>
- Simon P, Gogotsi Y (2008) Materials for electrochemical capacitors. *Nat Mater* 7(11):845–854. <https://doi.org/10.1038/nmat2297>
- Simon P, Gogotsi Y (2013) Capacitive energy storage in nanostructured carbon-electrolyte systems. *Acc Chem Res* 46(5):1094–1103. <https://doi.org/10.1021/ar200306b>
- Stoller MD, Park S, Zhu Y, An J, Ruoff RS (2008) Graphene-based ultracapacitors. *Nano Lett* 8(10):3498–3502. <https://doi.org/10.1021/nl802558y>
- Tanahashi I, Yoshida A, Nishino A (1990) Electrochemical characterization of activated carbon-fiber cloth polarizable electrodes for electric double-layer capacitors. *J Electrochem Soc* 137(10):3052–3057. <https://doi.org/10.1149/1.2086158>
- Thostenson ET, Ren Z, Chou T-W (2001) Advances in the science and technology of carbon nanotubes and their composites: a review. *Compos Sci Technol* 61(13):1899–1912. [https://doi.org/10.1016/S0266-3538\(01\)00094-X](https://doi.org/10.1016/S0266-3538(01)00094-X)
- Toupin M, Brousse T, Bélanger D (2004) Charge storage mechanism of MnO<sub>2</sub> electrode used in aqueous electrochemical capacitor. *Chem Mater* 16(16):3184–3190. <https://doi.org/10.1021/cm049649j>
- Vix-Guterl C, Frackowiak E, Jurewicz K, Friebe M, Parmentier J, Béguin F (2005) Electrochemical energy storage in ordered porous carbon materials. *Carbon* 43(6):1293–1302. <https://doi.org/10.1016/j.carbon.2004.12.028>
- Waller C, Luo D, Poon R, Zhitomirsky I (2017) Manganese dioxide-carbon nanotube composite electrodes with high active mass loading for electrochemical supercapacitors. *J Mater Sci* 52(7):3687–3696. <https://doi.org/10.1007/s10853-016-0711-0>
- Wang D-W, Li F, Zhao J, Ren W, Chen Z-G, Tan J, Wu Z-S, Gentle L, Lu GQ, Cheng H-M (2009) Fabrication of graphene/polyaniline composite paper via in situ anode electropolymerization for high-performance flexible electrode. *ACS Nano* 3(7):1745–1752. <https://doi.org/10.1021/nm900297m>

- Wang X, Liu J, Wang Y, Zhao C, Zheng W (2014a) Ni(OH)<sub>2</sub> nanoflakes electrodeposited on Ni foam-supported vertically oriented graphene nanosheets for applications in asymmetric supercapacitors. *Mater Res Bull* 52:89–95. <https://doi.org/10.1016/j.materresbull.2013.12.051>
- Wang X, Sun G, Routh P, Kim D-H, Huang W, Chen P (2014b) Heteroatom-doped graphene materials: syntheses, properties and applications. *Chem Soc Rev* 43(20):7067–7098. <https://doi.org/10.1039/C4CS00141A>
- Wang Z, Ogata H, Morimoto S, Ortiz-Medina J, Fujishige M, Takeuchi K, Muramatsu H, Hayashi T, Terrones M, Hashimoto Y, Endo M (2015) Nanocarbons from rice husk by microwave plasma irradiation: from graphene and carbon nanotubes to graphenated carbon nanotube hybrids. *Carbon* 94:479–484. <https://doi.org/10.1016/j.carbon.2015.07.037>
- Weinstein L, Dash R (2013) Supercapacitor carbons. *Mater Today* 10(16):356–357. <https://doi.org/10.1016/j.mattod.2013.09.005>
- Xiong G, Hembram KPSS, Reifenberger RG, Fisher TS (2013) MnO<sub>2</sub>-coated graphitic petals for supercapacitor electrodes. *J Power Sources* 227:254–259. <https://doi.org/10.1016/j.jpowsour.2012.11.040>
- Xu G, Ding B, Nie P, Shen L, Wang J, Zhang X (2013) Porous nitrogen-doped carbon nanotubes derived from tubular polypyrrole for energy-storage applications. *Chem Eur J* 19(37):12306–12312. <https://doi.org/10.1002/chem.201301352>
- Xu R, Wei J, Guo F, Cui X, Zhang T, Zhu H, Wang K, Wu D (2015) Highly conductive, twistable and bendable polypyrrole-carbon nanotube fiber for efficient supercapacitor electrodes. *RSC Adv* 2015(28):22015–22021. <https://doi.org/10.1039/C5RA01917F>
- Yan J, Fan Z, Wei T, Cheng J, Shao B, Wang K, Song L, Zhang M (2009a) Carbon nanotube/MnO<sub>2</sub> composites synthesized by microwave-assisted method for supercapacitors with high power and energy densities. *J Power Sources* 194(2):1202–1207. <https://doi.org/10.1016/j.jpowsour.2009.06.006>
- Yan S, Wang H, Qu P, Zhang Y, Xiao Z (2009b) RuO<sub>2</sub>/carbon nanotubes composites synthesized by microwave-assisted method for electrochemical supercapacitor. *Synth Met* 159(1-2):158–161. <https://doi.org/10.1016/j.synthmet.2008.07.024>
- Yan J, Fan Z, Wei T, Qian W, Zhang M, Wei F (2010) Fast and reversible surface redox reaction of graphene-MnO<sub>2</sub> composites as supercapacitor electrodes. *Carbon* 48(13):3825–3833. <https://doi.org/10.1016/j.carbon.2010.06.047>
- Yang Z, Zhang J, Kintner-Meyer MCW, Lu X, Choi D, Lemmon JP, Liu J (2011) Electrochemical energy storage for green grid. *Chem Rev* 111(5):3577–3613. <https://doi.org/10.1021/cr100290v>
- Yang Z, Ren J, Zhang Z, Chen X, Guan G, Qiu L, Zhang Y, Peng H (2015) Recent advancement of nanostructured carbon for energy applications. *Chem Rev* 115(11):5159–5223. <https://doi.org/10.1021/cr5006217>
- Yen H-F, Horng Y-Y, Hu M-S, Yang W-H, Wen J-R, Ganguly A, Tai Y, Chen K-H, Chen L-C (2015) Vertically aligned epitaxial graphene nanowalls with dominated nitrogen doping for superior supercapacitors. *Carbon* 82:124–134. <https://doi.org/10.1016/j.carbon.2014.10.042>
- Yoon B-J, Jeong S-H, Lee K-H, Kim HS, Park CG, Han JH (2004) Electrical properties of electrical double layer capacitors with integrated carbon nanotube electrodes. *Chem Phys Lett* 388(1–3):170–174. <https://doi.org/10.1016/j.cplett.2004.02.071>
- Young RJ, Lovell PA (2011) Introduction to polymers. CRC Press, Boca Raton
- Yu A, Chabot V, Zhang J (2013) Electrochemical supercapacitors for energy storage and delivery: fundamentals and applications. CRC Press, Boca Raton
- Zhai Y, Dou Y, Zhao D, Fulvio PF, Mayes RT, Dai S (2011) Carbon materials for chemical capacitive energy storage. *Adv Mater* 23(42):4828–4850. <https://doi.org/10.1002/adma.201100984>
- Zhang K, Zhang LL, Zhao XS, Wu J (2010) Graphene/polyaniline nanofiber composites as supercapacitor electrodes. *Chem Mater* 22(4):1392–1401. <https://doi.org/10.1021/cm902876u>
- Zhang K, Mao L, Zhang LL, On Chan HS, Zhao XS, Wu J (2011) Surfactant-intercalated, chemically reduced graphene oxide for high performance supercapacitor electrodes. *J Mater Chem* 21(20):7302–7307. <https://doi.org/10.1039/C1JM00007A>

- Zhao X, Tian H, Zhu M, Tian K, Wang JJ, Kang F, Outlaw RA (2009) Carbon nanosheets as the electrode material in supercapacitors. *J Power Sources* 194(2):1208–1212. <https://doi.org/10.1016/j.jpowsour.2009.06.004>
- Zhong C, Deng Y, Hu W, Qiao J, Zhang L, Zhang J (2015) A review of electrolyte materials and compositions for electrochemical supercapacitors. *Chem Soc Rev* 44(21):7484–7539. <https://doi.org/10.1039/c5cs00303b>
- Zhu Y, Murali S, Stoller MD, Ganesh KJ, Cai W, Ferreira PJ, Pirkle A, Wallace RM, Cychosz KA, Thommes M, Su D, Stach EA, Ruoff RS (2011) Carbon-based supercapacitors produced by activation of graphene. *Science* 332(6037):1537–1541. <https://doi.org/10.1126/science.1200770>